Solution and Gelling Properties of Gellan Benzyl Esters

Mariella Dentini,* Pasquale Desideri, and Vittorio Crescenzi

Department of Chemistry, "La Sapienza" University, 00185 Rome, Italy

Yoshiaki Yuguchi, Hiroshi Urakawa, and Kanji Kajiwara

Department of Material Science and Chemistry, Kyoto Institute of Technology, Kyoto, Sakyo-ku, Matsugasaki, 606-8585 Japan

Received May 19, 1999; Revised Manuscript Received August 16, 1999

ABSTRACT: Gellan benzyl esters of different degrees of esterification were prepared, and their gelation behavior was examined. Native gellan and gellan benzyl ester aqueous solutions and the ensuing aqueous gels obtained by cooling their solutions with added salt were studied by means of rheological and small-angle X-ray scattering experiments. Although esterification causes no fundamental changes in the gellan ordered structure, the introduction of bulky benzyl ester groups reduces the backbone propensity of double-helix formation and subsequent helix−helix association (gelation). In consequence, gellan-based gels become less stable both mechanically and thermally with esterification.

1. Introduction

Controlled esterification is for practically any polysaccharide a facile means to elicit novel properties or to modulate properties that are typical of the native structure, and thus it is of importance in both applied and basic studies. In this context, it was considered of interest to investigate the influence on solution and gelling properties of the bacterial polysaccharide gellan that the partial esterification of glucuronic acid moieties along the chains might bring about. To this end, a variable amount of benzylic groups was introduced in the gellan backbone by reacting the native polymer in the tetrabutylammonium salt form with benzyl bromide in dimethyl sulfoxide (DMSO).[1]

In a preliminary study, solution characteristics of gellan benzyl ester samples having different degrees of esterification were examined by means of circular dichroism spectroscopy.[1] For very low degrees of esterification, the thermal stability of gellan gels was found to decrease with increasing esterification. This implies a decrease of the ordered chain state (double-helix content) in aqueous solution, and hence, the gel setting point is shifted to higher concentration. A further increase of the degree of esterification suppresses the sol−gel transition, and the double-helical chain state becomes of marginal thermal stability only. When the degree of esterification exceeds 0.4, gellan benzyl esters are no longer water-soluble.

In the present work, structural and gel forming characteristics of gellan and gellan partial benzyl esters in aqueous solution have been investigated in details by means of rheological and small-angle X-ray scattering (SAXS) measurements. An attempt of quantitative interpretation by model calculations for the junction zones is given, and the crystalline structure as suggested by Chandrasekaran[5] is taken as a basis.

2. Experimental Section

Partial gellan benzyl esters were prepared from DMSO solutions of gellan tetrabutylammonium according to the procedure schematically shown in Figure 1.[1,2] The degree of esterification (DE) of benzyl esters was determined by HPLC of the BzOH released by saponification. The degree of esterification of one series of samples studied in this work was as follows: 0 (the reference, gellan tetrabutylammonium salt, coded as TMA), 0.09 (gellan benzyl ester, coded as GBZ09), and 0.25 (gellan benzyl ester, coded as GBZ25). These samples were used in the rheological measurements on gellan gel at 10 °C and in the small-angle X-ray scattering experiments at 10 and 60 °C. In another series, gellan benzyl esters samples were prepared having degrees of esterification of 0.01 (coded GBZ01) and 0.22 (coded GBZ22), respectively; these were employed for the characterization of aqueous gel formation as a function of temperature or as a function of polymer concentration.

The rheological behavior of TMA, GBZ01, and GBZ22 was studied in the process of gelation of the modified gellan aqueous solutions using the C14 Couette geometry of a Bohlin CS10 controlled-stress rheometer, by either lowering temperature or increasing polymer concentration. Hot polymer solutions at 90 ± 0.1 °C were mixed with an appropriate amount of salt solution and placed directly in the Couette geometry. A few drops of mineral oil were added in order to prevent evaporation of the solutions. The temperature was then lowered to 5 ± 0.1 °C at the rate of 1 °C/min. Gelation was monitored by determining the storage and loss moduli G' and G'', respectively, at 0.1 Hz with a nominal deformation of 0.01. The elastic modulus was measured for TMA, GBZ09, and GBZ25 gels at 10 ± 0.1 °C, with a nominal deformation of 2×10^{-3} and with variations in the polymer or the salt concentrations.

The synchrotron radiation small-angle X-ray scattering experiments on TMA, GBZ09, and GBZ25 in water or aqueous salt solutions (50 and 150 mM NaCl and 50 mM KCl) at 10 °C and 60 °C were performed at the BL10C of the Photon Factory, Tsukuba, Japan. An incident X-ray from synchrotron radiation was monochromatized to $\lambda = 0.149$ nm with a double-crystal monochromator and then focused to the sample cell position with a bent focusing mirror. The intensity of scattered X-rays was measured by a one-dimensional position-sensitive proportional counter (PSPC) positioned at the distance of 1 m from the sample. A flat glass sample cell of 0.2 cm path length was used where the windows were made of thin quartz plates of 20 μm in thickness. The sample temperature was controlled by circulating water of a constant temperature around sample holder.

* To whom all correspondence should be addressed.

10.1021/ma9907901 CCC: $18.00
Published on Web 10/05/1999

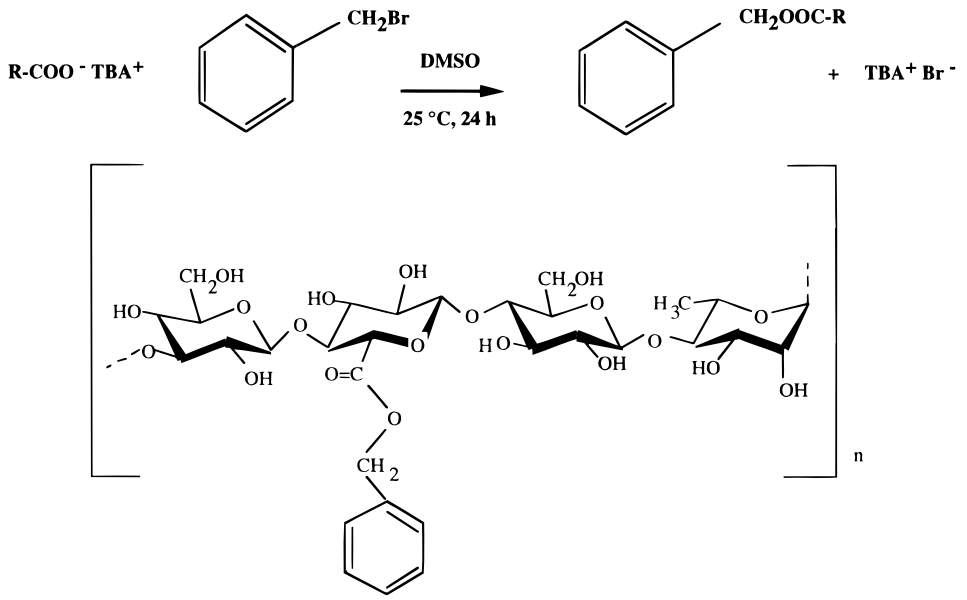

Figure 1. Preparation scheme and chemical structure of gellan benzyl ester.

Table 1. State of Gellan Benzyl Ester Aqueous Mixtures at 10 °C[a]

C_p	0.5[b]	1.5[b]	1.5[b]	1.5[b]	3[b]	6[b]
added salt	150[c]	0	50[c]	50[d]	0	0
TMA	G	S	G	G	G	G
GBZ09	G	S	S	G	S	G
GBZ25	G	S	S	G	S	S

[a] G = gel; S = sol. [b] $\times 10^2$ g cm^{-3}. [c] Millimoles of NaCl. [d] Millimoles of KCl.

3. Results and Discussion

3.1. Gelation Behavior. Gelation behavior of gellan and gellan benzyl ester derivatives is very dependent on the degree of esterification introduced in the chains, the polymer and salt concentration/cations, and the temperature. Experiments has been conducted in a carefully chosen range of the variables in order to point out the differences among gellan and its derivatives. TMA, GBZ09, and GBZ25 derivatives were dissolved in water by heating the solutions to 90 °C with stirring and the addition of standard NaCl or KCl aqueous solutions to obtain the desired final salt concentration (50 and 150 mM NaCl and 50 mM KCl). Gellan and its benzyl derivatives form clear solutions at 60 °C in any of the conditions examined.

The results concerning gelation behavior at 10 °C for TMA, GBZ09, and GBZ25 samples are summarized in Table 1, at polymer concentrations of 0.5, 1.5, 3 and 6 $\times 10^{-2}$ g/cm^3. TMA samples form gels by either increasing the polymer concentration from 1.5 $\times 10^{-2}$ to 3 $\times 10^{-2}$ g/cm^3 or adding salts (both cations). At low DE (GBZ09 samples), the polymer concentration useful to obtain gelation is shifted to the value of 6 $\times 10^{-2}$ g/cm^3 and gel is obtained at higher NaCl concentration (150 mM) or a more efficient gelation promoter like KCl (50 mM) must be used. At higher DE (GBZ25 samples), the polymer concentrations investigated are unable to induce gelation; gels are formed only by adding salts, in the same conditions as for GBZ09 derivative. In conclusion, gelation is promoted by adding KCl or NaCl or increasing the polymer concentration, whereas esterification tends to suppress it.

3.2. Rheological Characterization. The thermal development of elastic moduli was observed from the system of gellan benzyl ester (DE = 0.01) in 680 mM NaCl aqueous solution ($C_p = 0.45 \times 10^{-2}$ g/cm^3) while the temperature was decreased from 90 to 5 °C. The sol−gel transition was observed as a sharp increase of the storage modulus G' around 65 °C (see Figure 2). Below 60 °C, G' is much larger than G'' in the gel state.

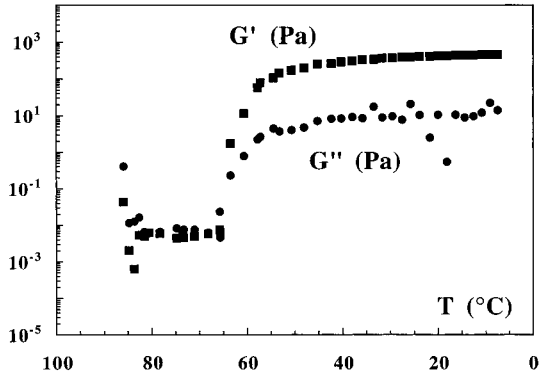

Figure 2. G' and G'' moduli evolution with temperature during gel setting for gellan−TMA−benzyl ester (GBZ01) at 0.1 Hz and 0.01 strain. ($C_p = 0.45 \times 10^{-2}$ g/cm^3, $C_{NaCl} = 680$ mM).

G' was measured with gels prepared in aqueous NaCl for different polymer concentrations with a salt-to−polymer equivalent ratio R (C_{salt}/C_p) fixed to 110. This ratio was adopted in order to have a homogeneous gel phase as deduced from previous optical measurements.[1] As seen from Figure 3, the concentration dependence of G' follows an expected behavior[3] with a sharp increase at the critical gel concentration and subsequent C_p^2 dependency above the critical point. G' of the parental gellan TMA seems to approach a limiting value at high polymer concentrations. At high concentrations of about 8 mg/cm^3, almost the same value for G' is observed, independent of esterification. Before reaching a limiting value, G' was found to decrease with increasing degrees of esterification. The critical gel concentration C_0 was estimated by extrapolation with a second-order polynomial fitting from Figure 3, and the values are reported as a function of esterification in Figure 4. The critical gel concentration C_0 increases with esterification, suggesting that esterification reduces the relative number

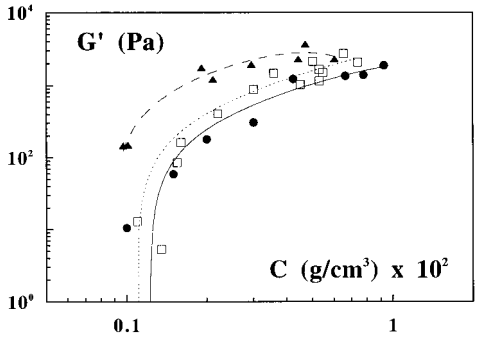

Figure 3. Polymer concentration dependence of G' for gellan−TMA and its benzyl ester gels at 5 °C, where the ratio of the salt-to−polymer concentration R is fixed to 110 (0.1 Hz, 0.01 strain). (▲): TMA, dashed line. (□): GBZ01, dotted line. (●): GBZ22, full line.

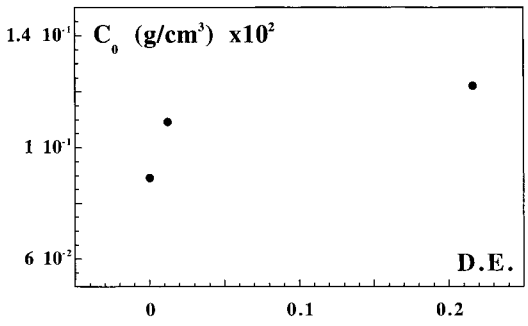

Figure 4. Extrapolated apparent critical gel concentration, C_0, from data in Figure 3 as a function of the degree of esterification for TMA, GBZ01, and GBZ22.

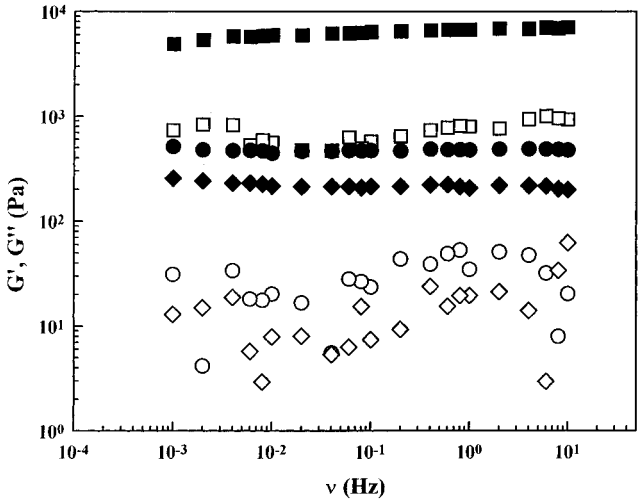

Figure 5. Mechanical spectra of TMA (■), GBZ09 (●), and GBZ25 (◆) in 150 mM NaCl. Polymer concentration: 0.5×10^{-2} g/cm^3 ($T = 10$ °C, 2×10^{-3} strain). Full symbols: G'. Open symbols: G''.

of physical cross-links. However, a common limiting value of G' at high concentrations indicates that the gel assumes, eventually, the same network structure regardless of esterification.

The gellan TMA benzyl ester samples used in SAXS measurements, namely TMA, GBZ09, and GBZ25, have been also tested by frequency sweeps at 10 ± 0.1 °C and 2×10^{-3} deformation in the range $\nu = 10^{-3} \div 10$ Hz (Figures 5 and 6). Results of experiments are summarized in Table 2.

The comparison with the TMA rheological behavior reveals a consistent decrease of moduli values as esterification proceeds. The use of NaCl instead of KCl allows a better discrimination of the different DE of the samples but reduces the range of operative salt concentrations. For example, no gelation takes place in 50 mM NaCl aqueous solutions of GBZ09 and GBZ25 (see Table 1).

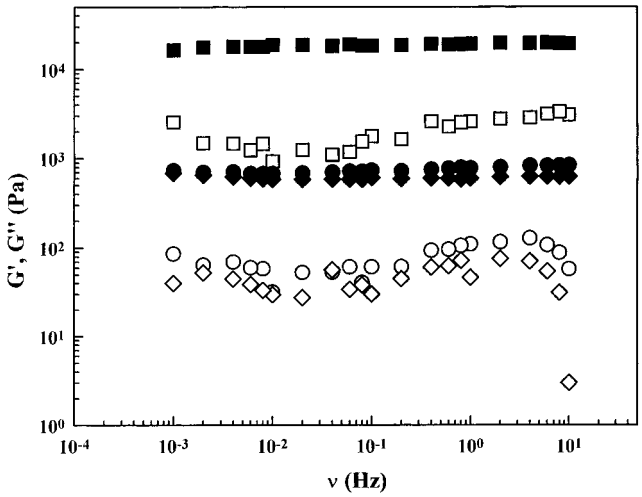

Figure 6. Mechanical spectra of TMA (■), GBZ09 (●), and GBZ25 (◆) in 50 mM KCl. Polymer concentration 1.5×10^{-2} g/cm^3 ($T = 10$ °C, 2×10^{-3} strain). Full symbols: G'. Open symbols: G''.

Table 2. G' and G'' Moduli at 10 °C, 0.1 Hz, and 2×10^{-3} Strain

code	C_p [a]	salt	G' (Pa)	G'' (Pa)
TMA	0.5	150 mM NaCl	6408	577
	1.5	50mM NaCl	2828	295
	1.5	50mM KCl	18575	1786
GBZ9	0.5	150mM NaCl	474	24
	1.5	50mM NaCl	no gel	no gel
	1.5	50mM KCl	742.5	61.5
GBZ25	0.5	150mM NaCl	214	7.5
	1.5	50mM NaCl	no gel	no gel
	1.5	50mM KCl	612	30

[a] $\times 10^{-2}$ g/cm^3

The decrease of the elastic modulus along with esterification may be ascribed to fewer available junction zones or longer effective network chains. Because gellan TMA benzyl ester gels eventually have the same network structure as gellan TMA gels regardless of the degree of esterification, as confirmed by the concentration dependence of G' (Figure 3), esterification does not completely suppress but merely weakens the double-helix formation and its subsequent association. This conjecture is consistent with the SAXS observation on the same systems.

3.3. Small-Angle X-ray Scattering. Three gellan samples, namely TMA, GBZ09, and GBZ25, were subjected to SAXS observation in aqueous solutions with and without added salt at 60 and 10 °C. Owing to its short wavelength, the SAXS is expected to provide structural information on the order of 10−1000 Å, which is supposed to be the order of fundamental distances responsible for the macroscopic structural change. The SAXS was observed from gellan benzyl esters in aqueous solution with variations in the ambient condition.

An example of the observed SAXS profile for 3.0×10^{-2} g/cm^3 TMA, GBZ09, and GBZ25 aqueous solution at two temperatures is shown in Figure 7a−c. The interference peak due to the electrostatic interaction between carboxyl groups was observed in all solutions

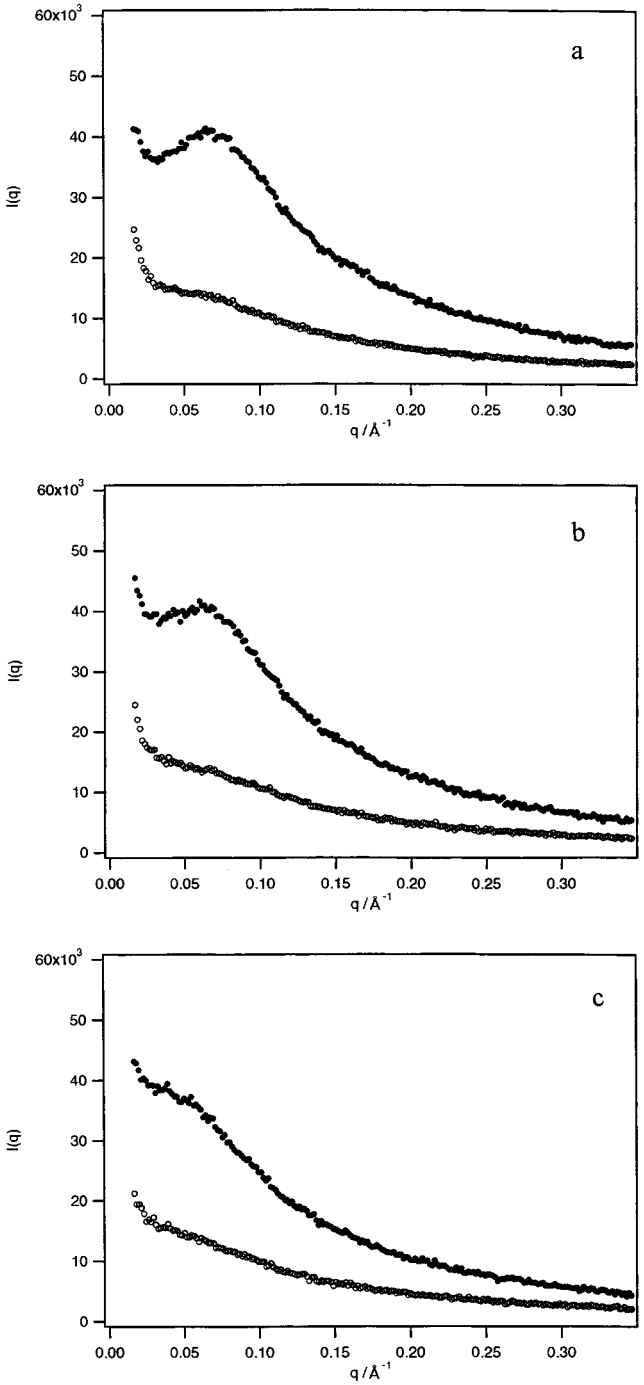

Figure 7. Observed SAXS profiles from 3.0×10^{-2} g/cm^3 TMA (a), GBZ09 (b), and GBZ25 (c) aqueous solutions at 10 (full symbols) and 60 °C (open symbols).

without salt, although the interference peak is less marked as the DE is increased. The salt efficiently screens the electric charges on the carboxyl groups and the interference peak disappears in the SAXS profile observed from the gellan solutions with added salt. Although the SAXS profile from the double helix exhibits a good linearity in the Guinier plot for a cross section[4] [$\ln(qI(q))$ vs q^2] as expected from its cylindrical shape, the bundle formed by aggregated double helices seems to be not rodlike but flat. Here, q denotes the magnitude of the scattering vector, given by $(4\pi/\lambda)\sin(\theta/2)$, with λ and θ being the wavelength of the incident beam and the scattering angle, respectively, and $I(q)$ being the scattered intensity. No good linearity was observed in the Guinier plot for a cross section of the SAXS data of TMA, GBZ09, and GBZ25 gels. Instead, the Guinier plot for thickness[4] ($\ln[q^2I(q)]$ vs q^2) revealed a good linearity, and a bundle thickness was evaluated from the slope as ca. 26.5 Å for all gellan gels. The evaluated thickness is considered to represent the thickness of the junction zones, which seem to be flat platelike. Here, although the respective Guinier plots yield directly the corresponding radius of gyration from the slope, the radius of gyration can be converted to the diameter of a cylinder or the thickness of a disk by assuming a homogeneous density of the object.[4]

Because the evaluated thickness (26.5 Å) corresponds to the double layer of packed double helices of gellan,[5] the results indicate that the gellan double helices associate in a double layer to form the junction zone as shown in Figure 8. The molecular models of associated double helices were constructed by following the crystallographic analysis of Chandrasekaran et al.[5]

A modified broken-rod model was applied to analyze the scattering profiles of gellan solutions and gels with the use of the molecular models for a single- or double-helical conformation,[6] according to the procedure described before.[7] We extend the analysis of the SAXS profiles in terms of the packing model of gellan molecules (Figure 8), which may elucidate the structural details of the junction zone.

The scattering profile is assumed to be represented by a modified broken-rod model[6−8] as

$$\frac{q^2I(q)}{c} \approx \sum_i q^2 w_i M_{L\,i} \Theta_i(q) + \text{const} \qquad (1)$$

Here, the subscript i denotes the ith component constituting a broken fragment in the modified broken-rod model. The broken fragment corresponds to either of the molecular models represented in Figure 8. $\Theta_i(q)$ is its corresponding particle scattering factor calculated from the atomic coordinates of the respective molecular models according to the Debye formula:

$$I(q) = \sum_{i=1}^{n} f_i^2\, g_i^2(q) + 2\sum_{i=1}^{n-1}\sum_{j=i+1}^{n} f_i f_j g_i(q) g_j(q) \frac{\sin(d_{ij}q)}{d_{ij}q} \qquad (2)$$

where f_i and d_{ij} denote the atomic scattering factor of the ith atom and the distance between the ith and jth atoms, respectively. The form factor $g_i(q)$ of a single atom is assumed to be represented by the form factor of a sphere possessing the radius equivalent to the van der Waals radius of the ith atom as

$$g_i(q) = \frac{3[\sin(R_iq) - (R_iq)\cos(R_iq)]}{(R_iq)^3} \qquad (3)$$

Here, R_i denotes the van der Waals radius of the ith atom and is set to 1.67 or 1.50 Å for a carbon or an oxygen atom, respectively. The constant term in eq 1 takes into account the interbroken-fragment correlation distributed randomly in the system. The constant term involves three factors: the first accounts for the number of fragment ends per unit length, the second accounts for the number of kinks per unit length, and the third accounts for the number of crossing per unit length with other fragments.[9]

To take into account the interference peak due to the electrostatic interactions, the scattering profile is as-

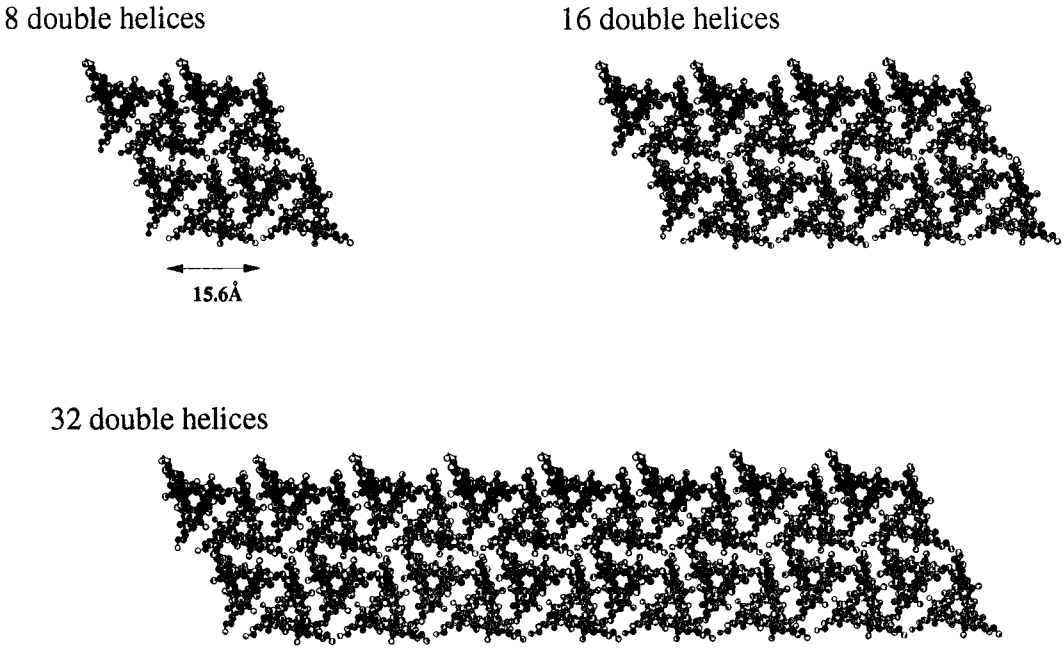

Figure 8. Packing model of gellan molecules. 32, 16, and 8 associated gellan double helices are supposed to form a junction zone.

sumed to be represented by the product of the form factor (the particle scattering factor) $P(q)$ of an isolated particle and the interference $S(q)$ as

$$I(q) \approx P(q)S(q) \tag{4}$$

The particle scattering factor is equivalent to eq 2 for an isolated noninteracting particle when the intensity is normalized with respect to the zero-angle intensity $I(0)$. The interparticular interaction should be isotropic in eq 4. This condition will be satisfied in solution, where the particles move fast enough to smooth the interaction potential in the form of a Gaussian function as $\exp(-r^2/\xi^2)$, where ξ denotes the correlation length of interaction as a measure of the distance decaying the interaction potential to 1/e.

Because the structure factor $S(q)$ is given by the Fourier transform of the interaction potential,[11] $S(q)$ will be expressed as[12]

$$S(q) = \frac{1}{1 + 2cA_2M_w e^{(-\xi^2q^2)}} \tag{5}$$

where A_2 denotes the second virial coefficient and is introduced by adjusting the second term in the virial expansion of eq 5 to the conventional expression.

The SAXS profiles are analyzed according to eq 1, where the interference was taken into account according to eq 4 when necessary. The example is shown in Figure 9 for 3.0×10^{-2} g/cm^3 TMA aqueous solution at 60 and 10 °C. Here, the interchain interaction due to the remaining carboxyl groups causes an interference peak. Taking into account the interchain interaction in terms of a Gaussian potential, the model calculation according to the modified broken-rod model was executed to fit to the observed SAXS profiles. Figure 9 indicates that the conformation of TMA in water at 60 °C seems to be represented by a single helix constructed by removing one chain from a gellan double helix. The electrostatic interaction is present and is specified by the correlation length of interaction of 21.0 Å. The TMA chains form a double helix at 10 °C, but the double-helical conformation is broken into parts because the constant term is required in the broken-rod model to fit to the observed SAXS profile (Figure 9). Because of the resolution of SAXS, the frequency of these breaks cannot be estimated except for the minimum length of the double-

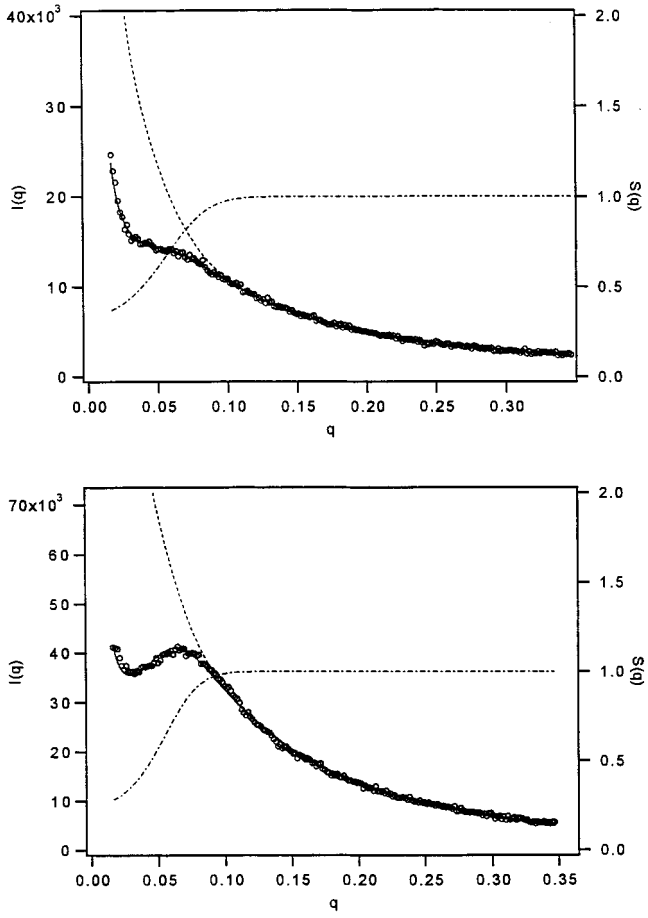

Figure 9. Observed SAXS profiles from 3.0×10^{-2} g/cm^3 TMA aqueous solution at 10 (bottom) and 60 °C (top), with profiles calculated according to eqs 1 and 4. $I(q)$: full line. $P(q)$: dotted line. $S(q)$: dash-and-dot line.

Table 3. Correlation Length of Interaction in Gellan and Its Benzyl Esters in Water

	1.5×10^{-2} g/cm^3		3×10^{-2} g/cm^3		6×10^{-2} g/cm^3	
code	10 °C	60 °C	10 °C	60 °C	10 °C	60 °C
TMA	27.5 Å	29.4 Å	23.4 Å	21.0 Å	15.4 Å	19.6 Å
GBZ09	26.0 Å	31.1 Å	24.0 Å	20.7 Å	18.7 Å	16.6 Å
GBZ25	23.9 Å	34.0 Å	23.1 Å	21.0 Å	22.9 Å	16.7 Å

Table 4. Weight Fraction of the Components of Associated Double Helices[a]

code	C_p[b]	salt	10 °C	60 °C
TMA	0.5	150 mM NaCl	32d(0.98) + 16d(0.02)	
	1.5	50 mM NaCl	3d(0.54) + 2d(0.10) + d(0.10) + s(0.26)	s(1)
	1.5	50 mM KCl	16d(0.68) + 2d(0.32)	s(1)
	1.5	0	d(0.42) + s(0.58)	s(1)
	3.0	0	d(1)	s(1)
	6.0	0	2d(0.77) + d(0.23)	s(1)
GBZ09	0.5	150 mM NaCl	32d(0.98) + 16d(0.02)	
	1.5	50 mM NaCl	2d(0.42) + d(0.39) + s(0.19)	s(1)
	1.5	50 mM KCl	16d(0.68) + 2d(0.35)	s(1)
	1.5	0	d(0.42) + s(0.58)	s(1)
	3.0	0	d(1)	s(1)
	6.0	0	2d(0.20) + d(0.80)	s(1)
GBZ25	0.5	150 mM NaCl	32d(0.76) + 16d(0.135) + 8d(0.105)	
	1.5	50 mM NaCl	2d(0.42) + d(0.39) + s(0.19)	s(1)
	1.5	50 mM KCl	32d(0.47) + 16d(0.34) + 2d(0.19)	s(1)
	1.5	0	d(0.14) + s(0.86)	s(1)
	3.0	0	d(0.72) + s(0.28)	s(1)
	6.0	0	2d(0.455) + d(0.455) + s(0.09)	s(1)

[a] 32d, 16d, 8d, 3d, 2d, d, and s denote 32, 16, 8, 3, and 2 double-helix associates, double helix, and single helix, respectively. (See Figure 8). [b] $\times 10^{-2}$ g/cm^3.

helical portion, which corresponds to the length of the present molecular model (84.6 Å, 18 saccharide units). Here, the rodlike portions consisting of gellan double helices are supposed to be freely jointed by short, disentangled single chains. The electrostatic interaction is more pronounced although the correlation length of interaction is in the same order (23.4 Å), indicating higher ion density on the double-helical parts.

A similar analysis was also applied to other systems in water solutions (without added salt). The results are summarized in Table 3. Gellan and its benzyl esters assume a single-helical conformation in all solutions at 60 °C. An electrostatic interaction is present in water solutions, where the correlation length of interaction decreases with increasing polymer concentration. With esterification, the electrostatic interaction becomes smaller but recognizable. At 10 °C, the chain assumes partially a double-helical conformation, but a single helical conformation is still present (see Table 4). In 6×10^{-2} g/cm^3 solution, the double helices associate in two parallel aligned double helices. TMA forms a gel in 6×10^{-2} g/cm^3 water solution at 10 °C, but no gelation took place in its benzyl esters. That is, gelation needs at least two double-helix associates, where no single helix should be present and the correlation length of interaction is less than 16 Å.

NaCl or KCl promotes the gel formation of gellan and its benzyl esters. TMA, GBZ09, and GBZ25 form thermoreversible gels in 50 mM KCl and 150 mM NaCl aqueous solution when the temperature is lowered to 10 °C. A clear peak is observed upon gel formation in

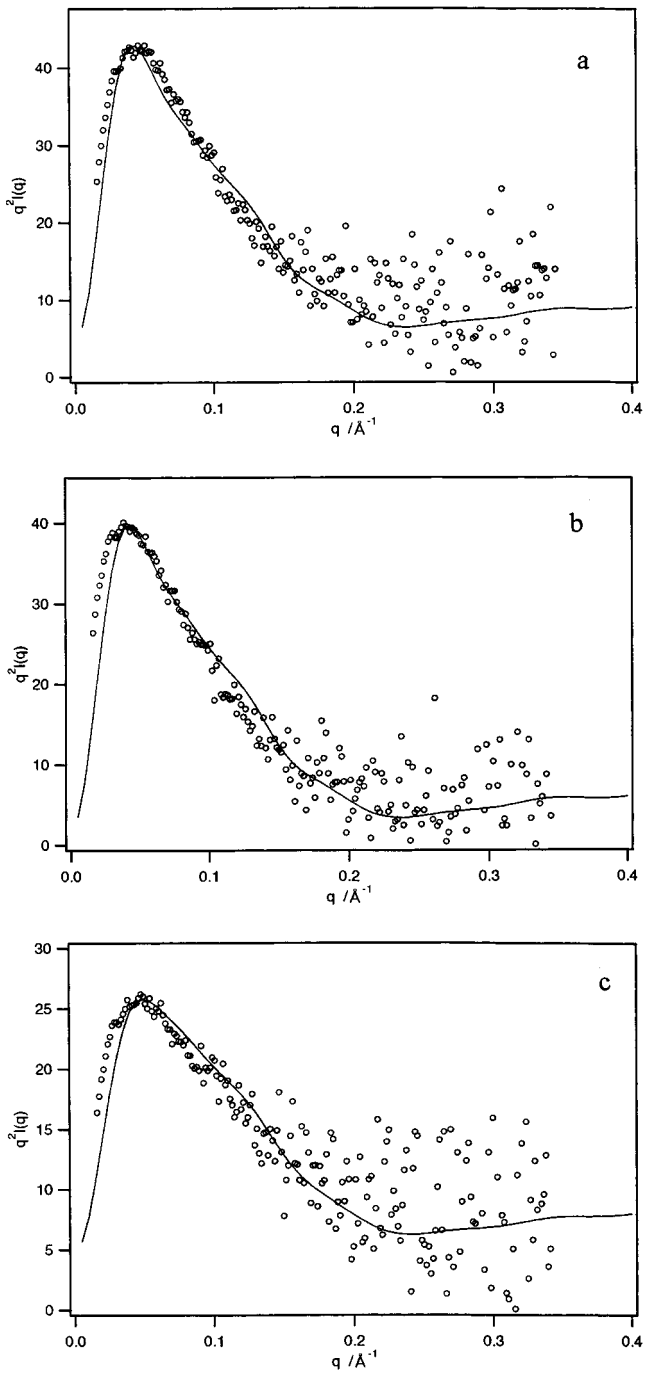

Figure 10. Observed SAXS profiles from TMA (a), GBZ09 (b), and GBZ25 (c) gels in 150 mM NaCl (at 10 °C) and the calculated scattering factors (solid lines) with a modified broken-rod model composed of the molecular models shown in Figure 8. Polymer concentration: 0.5×10^{-2} g/cm^3.

the Kratky plots of the experimental SAXS profiles. Because the electric charges are shielded by added salt, no interference appears in the SAXS profiles. The fraction of associated components was evaluated by fitting the scattering profiles calculated in eq 1 to the observed SAXS profiles, where the association of gellan double helices is assumed to proceed according to the scheme shown in Figure 8. The fitting example is shown in Figure 10 for TMA, GBZ09, and GBZ25 gels in 150 mM NaCl aqueous solution. Although the details of our model could not be confirmed, the following conclusion can be drawn about the numbers of double helices that associate to make junction zones. The highest degree

of association was achieved in 150 mM NaCl aqueous solution, where gellan would associate into 32 double helices aligned in a double layer.

In water without added salt, esterification suppresses double-helix formation in gellan. The double helices are eventually formed by adding salt or increasing the polymer concentration. However, the lower degree of association is favored in higher esterified gellan. For example, in the present model analysis, gellan associates into three double helices in 50 mM NaCl aqueous solution, but the maximum number of association reduces to two by esterification. Esterification is expected to reduce the number of interchain ionic interactions stabilizing gellan double helices and to disfavor chain pairing. Even when the double helices are formed, the double helices involving bulky benzyl esters associate less tightly because the interhelix distance is larger by 0.4 Å in the gellan benzyl ester crystal.[10] It might be the case that the domain composed of associated double helices is loosely packed in GBZ25. Here, a large number of benzyl groups sticking out of the double helix require space to be accommodated, so that the interhelix distance evaluated crystallographically is larger than 0.4 Å. This tendency was observed as the shift of gel−sol transition to a lower temperature by esterification.[1]

Esterification makes associated double helices more vulnerable to breakage by external stimuli. However, the formation of double helices and their subsequent associations are common, and the structure of associated domains is the same in high salt and polymer concentrations regardless of esterification.

4. Conclusions

Gellan and its benzyl ester derivatives form aqueous gels by adding salt or increasing polymer concentration. Here, the cross-linking domain is constituted of associated double helices in a double layer in both gellan and gellan benzyl ester gels. Although the network structure appears to be the same regardless of esterification, the cross-linking domain becomes less complex and more vulnerable to breakage by external stimuli with increasing degrees of esterification.

However, with increasing benzylation, hydrophobicity is strongly increased. Thus, another type of association or cluster formation may have taken place that has not yet been taken into account in this study.

Acknowledgment. This work has been partially carried out with financial support from the Italian National Research Council "Bilateral Project" and the Italian Ministry for Universities and Research (MURST). M.D. is indebted to the Kyoto Institute of Technology for a Visiting Professorship at the Department of Materials Science and Chemistry. K.K. thanks "La Sapienza" University, the Japanese Society for Promoting Science, and the Italian National Research Council Bilateral Project for financial support. The SAXS measurements were performed under the approval of the Photon Factory Advisory Committee (Proposal No. 94G291).

References and Notes

(1) Crescenzi, V.; Dentini, M.; Maschio, S.; Segatori, M. *Makromol. Chem. Macromol. Symp.* **1993**, *76*, 95−97.
(2) Crescenzi, V.; Dentini, M.; Sergatori, M.; Tiblandi, C.; Callegaro, L.; Benedetti, L. *Carbohydr. Res.* **1992**, *231*, 73−81.
(3) Clark, A. H.; Ross-Murphy, S. B. *Adv. Polym. Sci.* **1987**, *83*, 57−192.
(4) *Small-Angle X-ray Scattering*; Glatter, O., Kratky, O., Eds.; Academic Press: London, 1982.
(5) Chandrasekaran, R.; Puigjaner, L. C.; Joyce, K. L.; Arnott, S. *Carbohydr. Res.* **1988**, *114*, 181−187.
(6) Yuguchi, Y.; Urakawa, H.; K. Kajiwara, *Macromol. Symp.* **1997**, *120*, 77−89.
(7) Coviello, T.; Maeda, H.; Yuguchi, Y.; Urakawa, H.; Kajiwara, K.; Dentini, M.; Crescenzi, V. *Macromolecules* **1998**, *31*, 1602−1607.
(8) Guenet, J.-M. *Thermoreversible Gelation of Polymers and Biopolymers*; Academic Press: London, 1992.
(9) Luzzati, V.; Benoit, H. *J. Appl. Crys.* **1961**, *14*, 297−300.
(10) Chandrasekaran, R.; Le, E. J.; Radha, A.; Thailambal, V. G. In *Frontiers in Carbohydrate Research 2*; Chandrasekaran, R., Ed; Elsevier Applied Science: London; 1992; p 65.
(11) Guinier, A.; Fournet, G. *Small-Angle Scattering of X-rays;* John Wiley: New York, 1955; p 43.
(12) Ikeda, Y.; Murakami, T.; Yuguchi, Y.; Kajiwara, K. *Macromolecules* **1998**, *31*, 1246−1953

MA9907901